# Amplification of linear strain in a layer excited by a shear-wave earthquake pulse

V. Gicev [a], M.D. Trifunac [b,*]

[a] Fakultet za informatika, University Goce Delčev, 2000 Štip, Republic of Macedonia
[b] Department of Civil Engineering, University of Southern California, Los Angeles, CA 90089, USA

## ARTICLE INFO

## ABSTRACT

Peaks of transient strains in a layer over semi-infinite half space are amplified by interference during up- and down-propagating waves, and they depend upon the impedance ratio of the layer and of the half space, as well as the wavelength. The amplification of incident motion on the ground surface is usually described in the frequency space for the response to a steady state, periodic excitation. To understand how this amplification develops for transient responses and for applications in which the linear theory leads to satisfactory answers, this paper describes the amplification in time in a layer excited by a shear-wave pulse. It is shown that the maximum amplification is equal to 2 for a "stiff" layer on a "soft" half space, and equal to 4 for a "soft" layer on a "stiff" half space, when the layer thickness corresponds to the quarter wavelength of the wave in the layer.

## 1. Introduction

With exception of soft (low-velocity) and cohesionless soils, most sites at moderate and large distances from earthquakes respond to shaking by intermediate and small earthquakes in essentially a linear manner. Analyses of the repeated recordings at the same strong-motion stations and of multiple recordings in the near field show that the strains smaller than approximately $10^{-5}$, in typical soils, can be described by the linear theory [27,28,32,33].

In this paper we present closed-form solution for the amplification of strains in a layer over half space subjected to half-sine pulse, assuming linear deformations and no damping. The response of a layer over half space subjected to seismic waves is a well-studied subject in a large number of papers and textbooks (e.g. [2,1,10]). Wave-propagation methods in earthquake engineering analyses of the linear response of soil layers and of buildings have been used since the 1930 s [16,17,8,9]. In the following, the elementary aspects of wave propagation through a homogeneous shear layer will be used to study the relationships among the amplitudes of incident pulses and of the layer response, with emphasis on amplification of transient linear strains. One-dimensional (1-D) representation of shear waves will be used [18,13–15]. Because this model also describes shear waves in wide buildings (where the rocking response associated with soil-structure interaction can be neglected), some of the results of this analysis will also be useful for understanding the elementary aspects of nonlinear response of such buildings [4,5].

Gičev and Trifunac [7] describe the behavior of the same physical model as in this paper, but for large pulse amplitudes, and for nonlinear response, for the assumed bi-linear stiffness representation of the soil. The present study complements that work and extends it to small amplitudes of excitation.

## 2. Model

We consider horizontal shear deformations, $u$, in a 1-D model of soil layer supported by a half space and excited by a vertically propagating shear wave represented by a half-sine pulse (Fig. 1). The linear equation of motion for this problem is

$$v_t = (\sigma)_x / \rho, \tag{1a}$$

and the relation between the derivative of the strain and the velocity is

$$\varepsilon_t = v_x, \tag{1b}$$

where $v$, $\rho$, $\sigma$, and $\varepsilon$ are particle velocity, density, shear stress, and shear strain, respectively, and the subscripts $t$ and $x$ represent derivatives with respect to time and space.

The domain for analysis consists of two materials (Fig. 1a): (1) $x < 0$, with physical properties $\rho_s$ and $\beta_s$, representing the half space, and (2) $0 < x \leq H_b$, with physical properties $\rho_b$ and $\beta_b$, representing the soil layer. $v = \partial u / \partial t$ and $\varepsilon = \partial u / \partial x$ are the velocity and the strain at a point, and $u$ is out-of-plane displacement of a particle perpendicular to the propagation ray. It is assumed that
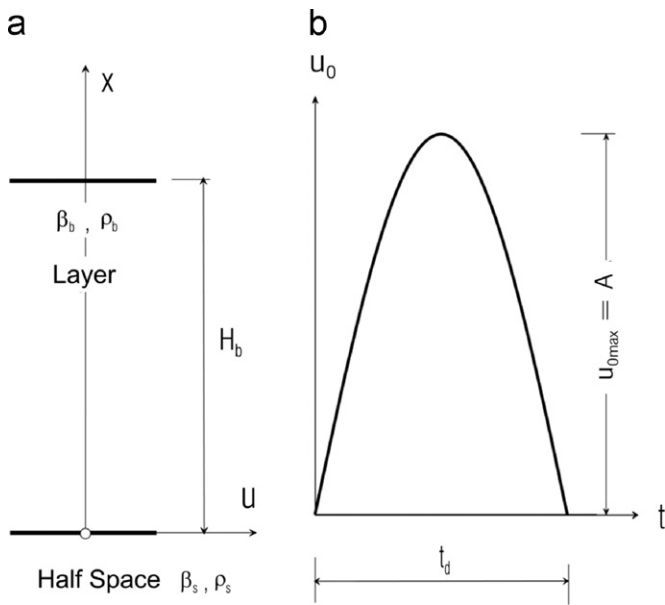
**Fig. 1.** Soil layer and incoming strong-motion displacement pulse: (a) model of the soil layer and (b) the pulse in the half space.

the incoming wave is known and that its displacement as a function of $t$ is prescribed, as in Fig. 1b. It consists of a single half-sine pulse, with peak displacement amplitude $A$ and duration $t_d$, and it propagates with velocity $\beta_s$

$$u_0 = A\sin\frac{\pi}{t_d}\left(t-\frac{x}{\beta_s}\right)\left[H\left(t-\frac{x}{\beta_s}\right)-H\left(t-\frac{x}{\beta_s}-t_d\right)\right],\qquad(2)$$

where $H$ is the step function.

The half-wavelength of this pulse is $L_w = t_d\beta_s$.

Following [5] and [7], the linear displacement and the strain in the linear layer are

$$u(x,t) = A\sum_{j=1}^{\infty}k_j\left\{\sin\frac{\pi}{t_d}\left(t-t_{j-1}-\frac{x}{\beta_b}\right)\left[H\left(t-t_{j-1}-\frac{x}{\beta_b}\right)-H\left(t-t_{j-1}-\frac{x}{\beta_b}-t_d\right)\right]+\right.$$
$$\left.+\sin\frac{\pi}{t_d}\left(t-t_j+\frac{x}{\beta_b}\right)\left[H\left(t-t_j+\frac{x}{\beta_b}\right)-H\left(t-t_j+\frac{x}{\beta_b}-t_d\right)\right]\right\}$$
$$(3)$$

and

$$\varepsilon(x,t) = A\frac{\pi}{\beta_b t_d}\sum_{j=1}^{\infty}k_j\left\{-\cos\frac{\pi}{t_d}\left(t-t_{j-1}-\frac{x}{\beta_b}\right)\left[H\left(t-t_{j-1}-\frac{x}{\beta_b}\right)-H\left(t-t_{j-1}-\frac{x}{\beta_b}-t_d\right)\right]\right.$$
$$\left.+\cos\frac{\pi}{t_d}\left(t-t_j+\frac{x}{\beta_b}\right)\left[H\left(t-t_j+\frac{x}{\beta_b}\right)-H\left(t-t_j+\frac{x}{\beta_b}-t_d\right)\right]\right\},$$
$$(4)$$

where $j$ is the order number of the passage of the wave along the path bottom-top-bottom in the layer, $t_j = 2jH_b/\beta_b$ ($j=0,1,2,3,....,$) is the time required for the wave to pass $j$ times along the path bottom-top-bottom (two heights), and

$$k_j = k_t k_r^{j-1}\qquad(5)$$

is the amplitude factor of the pulse in the half space during its $j$th passage along the path bottom–top–bottom through the layer, with $k_t$ and $k_r$ determined by the continuity of the displacements and stresses at the contact. For a transmitted wave from medium B to medium A, and for a reflected wave from medium A back into medium B, these coefficients are

$$k_{trB\to A} = 2[1+(\rho_a\beta_a)/(\rho_b\beta_b)]^{-1}\qquad(6)$$

and

$$k_{refB\to B} = [1-(\rho_a\beta_a)/(\rho_b\beta_b)]/[1+(\rho_a\beta_a)/(\rho_b\beta_b)].\qquad(7)$$

For the opposite direction of propagation, the numerators and the denominators in these fractions exchange places.

The odd terms in the series of Eq. (3) and Eq. (4) describe the response to the pulse coming from below, while the even terms describe the response for the pulse arriving from above. To describe this response in dimensionless terms, and to maintain continuity in notation with our previous studies (dealing with nonlinear layer response, [4,5,7]), in the following we will use the following dimensionless parameters:

dimensionless amplitude $\alpha = A/(H_b\cdot\varepsilon_{yb})$,  (8)

where $A$ is the amplitude of the pulse (Fig. 1b), $H_b$ the thickness of the layer, and $\varepsilon_{yb}$ the yielding strain in the layer, and

dimensionless frequency $\eta = 2H_b/\lambda_b = 2H_b/(\beta_b\cdot 2t_d) = H_b/(\beta_b\cdot t_d)$,
$$(9)$$

where $\lambda_b$ is the wavelength of the wave in the layer, $\beta_b$ the shear-wave velocity in the layer, and $t_d$ the duration of the incident wave represented by a half-sine pulse (Fig. 1b).

## 3. Analysis

### 3.1. Limits of linear response

To describe the amplitude-frequency space in which the layer response remains linear, we describe the limits of linear strain response (following [7]).

The constant that multiplies the series in Eq. (4) in terms of dimensionless amplitude and dimensionless frequency is

$$A\pi/(\beta_b t_d) = A_\varepsilon = \pi\alpha\eta\varepsilon_{yb}.\qquad(10)$$

To determine the limits of linear strain, we consider two fictitious points in the layer: (1) point B ($x=0$) at the layer-half space interface, and (2) point T ($x=H_b-\beta_b t_d/2$), where the amplitudes of the strain with the same sign meet after reflection from the top of the layer. To find the location of this point, we use Eq. (4). Its first term is 1 if the argument of the cosine function is equal to $t_d$ ($t-t_0-x/\beta_b=t_d$), and the second term is 1 if the argument of the second cosine function is equal to 0 ($t-t_1+x/\beta_b=0$). We then solve the system of two equations for $x$ and $t$ for $t_0=0$ and $t_1=2H_b/\beta_b$.

The position of T, where the strain amplitude is two times larger than the strain entering the beam, is at $x=H_b-\beta_b\cdot t_d/2$, and the time when this occurs is $t=H_b/\beta_b+t_d/2$. From Eq. (4), during the first passage of the pulse, $t<2H_b/\beta_b$, and at point B only the first term in the series exists. The strain at point B reaches its absolute maximum at the very beginning, during the entrance of the pulse into the layer, and its value is

$$|\varepsilon_{Bmax}^1| = \pi\alpha\eta\varepsilon_{yb}k_t.\qquad(11)$$

The condition for the strain at this point, to remain linear, is $|\varepsilon_{Bmax}^1|<\varepsilon_{yb}$, or, in terms of the dimensionless parameters assuming $\rho_b=\rho_s$

$$\alpha\eta < (\pi k_t)^{-1} = (\beta_b+\beta_s)/(2\pi\beta_s) = C_B.\qquad(12B)$$

At point T (this point does not exist if $t_d>2H_b/\beta_b$, and it coincides with point B if $t_d=2H_b/\beta_b$), from Eq. (4), the maximum strain during the first passage occurs at $t=H_b/\beta_b+t_d/2$, and its amplitude is $2A_\varepsilon\cdot k_t$. The condition for the strain to remain linear is

$$\alpha\eta < (2\pi k_t)^{-1} = (\beta_b+\beta_s)/(4\pi\beta_s) = C_T = C_B/2.\qquad(12T)$$

For example, for the shear-wave velocities $\beta_s = 250$ m/s, and $\beta_b = 100$ m/s, and $\rho_s = \rho_b = 2000$ kg/m$^3$, we find that $C_B = 0.2228$ and $C_T = 0.1114$.

When the reflected wave from the top of the layer reaches the soil-half-space interface ($t = t_1$), the wave begins the second passage. The linear solution for the strain in Eq. (4) at B now involves three terms in the series if the duration of the pulse is longer than $2H_b/\beta_b$, and two terms for shorter pulses. The solution at time $t = 2H_b/\beta_b = t_1$ is

$$\varepsilon(0, t_1) = A_\varepsilon\{k_1[-\cos(2\pi H_b/(\beta_b t_d)) + \cos 0] - k_2 \cdot \cos 0\} \quad (13a)$$

or

$$\varepsilon(0, t_1) = \pi\alpha\eta\varepsilon_{yb}k_t(1 - \cos 2\pi\eta - k_r) \quad (14a)$$

when $t_d > 2H_b/\beta_b$ ($\eta < 1/2$), and

$$\varepsilon(0, t_1) = A_\varepsilon\{k_1 \cdot \cos 0 - k_2 \cdot \cos 0\} \quad (13b)$$

or

$$\varepsilon(0, t_1) = \pi\alpha\eta\varepsilon_{yb}k_t(1 - k_r) \quad (14b)$$

when $t_d < 2H_b/\beta_b$ ($\eta > 1/2$).

Comparing Eq. (11) and Eq. (14b), because in our example $k_r < 0$, for short pulses ($\eta > 0.5$) the strain at point B at the beginning of the second passage is always larger ($(1 + |k_r|)$), and thus for our example (with $\beta_s = 250$ m/s, $\beta_b = 100$ m/s, and $\rho_s = \rho_b = 2000$ kg/m$^3$) it is 10/7 times larger than the strain $A_\varepsilon \cdot k_t$ at the beginning of the first passage—but it is smaller than the strain at T in the first passage ($2A_\varepsilon \cdot k_t$). For short pulses ($\eta > 0.5$), if there is no occurrence of permanent strain during the first passage at point T, the response of the layer will be linear for all time.

For long pulses ($\eta < 0.5$), comparing Eq. (11) and Eq. (14a), and for $\eta < (2\pi)^{-1}\arccos(|k_r|)$, the strain at interface point B at the beginning of the second passage is smaller than the strain at the beginning of the first passage, and for $\eta > (2\pi)^{-1}\arccos(|k_r|)$ the former strain is larger than the later one. For our example, ($k_r = -3/7$), and $\eta > 0.18$ always gives larger strain at the interface point at the beginning of the second passage than the strain at the beginning of the first passage.

The largest amplification of the strain at B is for $\eta = 0.5$ (see Eq.14a), when, at the beginning of the second passage, the strain is $(2 + |k_r|)$ times larger than the strain during the first passage. In our example, the amplification is 17/7, and this gives a larger strain than the strain at point T during the first passage ($2A_\varepsilon \cdot k_t$). Therefore, for long pulses ($\eta \leq 0.5$) the first exceeding of $\varepsilon_{yb}$ can occur later in time. This means that in addition to conditions (12B) and (12T) there is one further condition for the strain to remain linear, which is valid only in Zone 1, namely

$$\alpha\eta < \frac{1}{\pi k_t(2 + |k_r|)} = \frac{\beta_b + \beta_s}{2\pi\beta_s(2 + |k_r|)} = \frac{C_B}{2 + |k_r|}. \quad (12B2)$$

In further discussions, the region ($\eta, x$) will be divided into three sub-regions (zones):

Zone 1: $Z_1 = \{(\eta, x) | \eta < 0.5, \forall x\}$,
Zone 2: $Z_2 = \{(\eta, x) | 0.5 \leq \eta, x \sim 0\}$, and
Zone 3: $Z_3 = \{(\eta, x) | 0.5 \leq \eta, x > 0\}$.

Most of the discussion in this paper will be related to Zone 1, where $\eta = 2H_b/\lambda_b = 2H_b/(\beta_b \cdot 2t_d) = H_b/(\beta_b \cdot t_d) < 0.5$, for excitation by pulses with long waves.

In the following, we consider the normalized maximum strain in the layer, $\varepsilon_{max}$. This strain is the absolute maximum of the strain occurring in the layer at any time of its response. To represent it in dimensionless terms, we consider the quantity $v_{lin} = v_{entr}^{lin}$, which is the maximum linear velocity entering the layer:

$$v_{lin} = \pi A \cdot k_t/t_d = \pi\alpha\eta\varepsilon_{yb}\beta_b k_t. \quad (15)$$

Then, instead of describing the absolute maximum of the strain, we will consider the normalized maximum strain

$$\overline{\varepsilon}_{norm} = \varepsilon_{max}\beta_b/v_{lin} = \varepsilon_{max}/\varepsilon_{lin} \quad (16)$$

### 3.2. Maximum strains

The maximum value of the strain for the impedance ratio in our example occurs *at the beginning of the second passage* of the wave at time $t_{1+} = t_1 + \delta$ for $t_d = t_1$, where $\delta > 0$, $\delta \ll t_1$, and $t_1 = \frac{2H}{\beta_b}$. Using (Eq. (4)), we find that

$$\varepsilon(0, t_{1+}) = A_\varepsilon\{k_1(-\cos\pi + \cos 0) + k_2(-\cos 0)\}, \quad (17)$$

where $A_\varepsilon = \frac{A\pi}{\beta_b t_d} = \frac{v_s}{\beta_b}$, and $v_s$ is the velocity of the pulse in the half space.

Replacing $k_j = k_t \cdot k_r^{j-1}$ in (17) we obtain the linear strain at the beginning of the second passage

$$\varepsilon(0, t_{1+}) = A_\varepsilon \cdot k_t(2 - k_r). \quad (18)$$

Dividing Eq. (18) by $A_\varepsilon \cdot k_t = \frac{v_s k_t}{\beta_b} = \frac{v_{entr}^{lin}}{\beta_b} = \varepsilon_{lin}^0$ (amplification of the entry strain), at the beginning of the second passage of the wave on the path bottom–top–bottom, we obtain

$$\overline{\varepsilon_2} = 2 - k_r \quad (19)$$

For values in our example, the amplification is $\overline{\varepsilon}_2 = 2.428$.

A question arises as to whether the amplification of the entry strain is the largest at the beginning of the second passage for any impedance ratio ($r = \rho_s\beta_s/\rho_b\beta_b$)—remembering that the wave amplitude is decreased every time it encounters the boundary between the layer and the half space. To explore this, we again use Eq. (4), and obtain

$$\varepsilon(0, t_{2+}) = A_\varepsilon\{k_1\cos\pi + k_2(-\cos\pi + \cos 0) + k_3(-\cos 0)\}. \quad (20)$$

Replacing $k_j = k_t \cdot k_r^{j-1}$ ($j = 1,2,3,\ldots$) in Eq. (20) for the strain *at the beginning of the third passage*, we get

$$\varepsilon(0, t_{2+}) = A_\varepsilon k_t(-1 + 2k_r - k_r^2) = -A_\varepsilon k_t(1 - k_r)^2. \quad (21)$$

Dividing Eq. (21) by $\varepsilon_{lin}^0$, we obtain the amplification at the beginning of the third passage as

$$\overline{\varepsilon_3} = -(1 - k_r)^2. \quad (22)$$

Comparing Eqns. (22) and (19) for

$$\left|\frac{\overline{\varepsilon_3}}{\overline{\varepsilon_2}}\right| = \frac{(1 - k_r)^2}{2 - k_r} > 1, \quad (23)$$

the amplification of the entry strain at the beginning of the third passage is larger than the one at the beginning of the second passage. The solution of Eq. (23) is

$$k_r < \frac{1 - \sqrt{5}}{2} \quad \text{and} \quad k_r > \frac{1 + \sqrt{5}}{2}. \quad (24)$$

But the reflection coefficient of the wave coming from the layer toward the boundary between the layer and the half space is

$$k_r = \frac{1 - r}{1 + r}, \quad \text{where} \quad r = \frac{\rho_s\beta_s}{\rho_b\beta_b} \geq 0. \quad (24a)$$

This implies that $k_r \leq 1$ for any value of $r$, so the second branch $k_r > \frac{1+\sqrt{5}}{2}$ of the solution (24) is physically not possible.

Replacing $k_r$ from Eq. (24a) and solving Eq. (24), we obtain $\frac{1-r}{1+r} < \frac{1-\sqrt{5}}{2} = -0.618$, and

$$r > 4.236. \quad (25)$$

For these values of the impedance ratio r, the amplification at the beginning of the third passage is larger than the amplification at the beginning of the second passage.

Finally, we compare the amplification at the beginning of the second passage ($t = t_{1+}$) with the one at the end of the first passage ($t = t_{1-}$). For $t = t_{1-}$ the term $A_\varepsilon k_2(-\cos 0)$ in Eq. (17) vanishes, so the amplification of the entry strain *at the end of the*

*first passage* is

$$\overline{\varepsilon_{1e}} = 2. \tag{26}$$

This means that the wave still has not reached the contact, and thus we have a contribution only from the interference of the up-going and down-going parts of the wave. Comparing Eq. (26) with Eq. (19), we conclude that for positive $k_r$ ($r < 1$) the amplification is larger at the end of the first passage.

From the above we can describe the amplification of the entry strain as a function of the impedance ratios in Zone 1 ($\eta < 0.5$) for pulse duration $t_d = t_1$.

1. For impedance ratio $r < 1$ (the layer is stiffer than the half space), the largest amplification occurs at the end of the first passage of the wave before it hits the contact between the layer and the half space, and the normalized strain is $\overline{\varepsilon_1} = 2$.
2. For impedance ratios in the interval $1 < r < 4.236$, the largest amplification occurs at the beginning of the second passage of the wave just after the down-going wave has hit the contact between the soil layer and the half space, and the strain is $\overline{\varepsilon_2} = 2 - k_r = 2 - \frac{1-r}{1+r}$.
3. For impedance ratios $r > 4.236$, the largest amplification occurs at the beginning of the third passage of the wave just after the down-going wave has hit the contact between the layer and the half space, and its value is $(1 - k_r)^2 = \left(\frac{2r}{1+r}\right)^2$.

The above relations are summarized in Fig. 2. In Fig. 3, we show the results for a wide range of impedance ratios, $10^{-4} \le r \le 10^4$ and
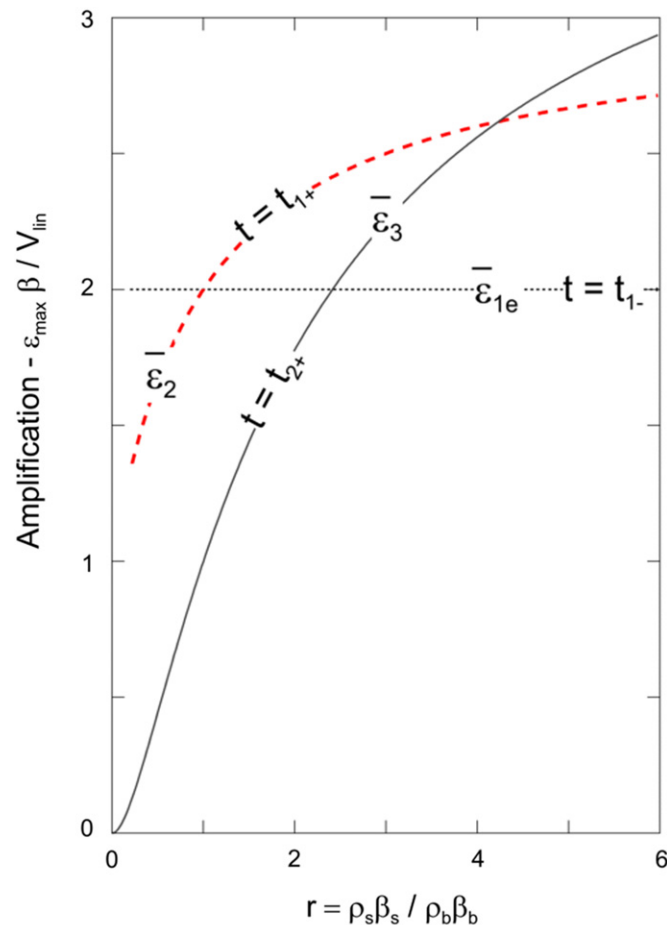
for 19 values of $\eta$. As can be seen from Fig. 3, for $\eta \ge 0.5$ the curves for any impedance ratio have a constant value equal to two. For these values of $\eta$, the wave is shorter than the double height of the layer. The maximum strain appears during the first passage, in Zone 3, and it results from the interference of the part of the wave going up and the part of the wave going down. Setting to zero the partial derivatives of the strain (Eq. (4)) with respect to time and space, we find that the largest strain occurs at $t_{\max} = \frac{H}{\beta} + \frac{t_d}{2}$, at the point $x_{\max} = H - \frac{\beta \cdot t_d}{2}$. These values correspond to an instant when the front of the wave going downward and the tail of the wave going upward meet.

For small dimensionless frequencies, $0.01 \le \eta \le 0.07$ (long waves), the amplification of the strain is approximately symmetric with respect to $r = 1$ ($\log_{10} r = 0$). As $r$ approaches zero or infinity, the amplification of the strain approaches 2 (Fig. 3).

For larger dimensionless frequencies in Zone 1, $0.1 \le \eta < 0.5$, except that for $\eta = 0.1$ in our examples in Fig. 3, as $r$ becomes large, the amplification of the strain is larger than 2 and increases with increasing $\eta$. For large impedance ratios, the coefficient of reflection of the wave from the bottom of the layer boundary back into the layer is $k_r = \lim_{r \to \infty} \frac{1-r}{1+r} = -1$. As we saw above, the amplification at the beginning of the third passage is $(1 - k_r)^2$, and the largest amplification in the first zone approaches 4. For $\eta = 0.4999$, the analytical solution of the amplification is essentially 4.

To explain why the above trend is not observed for $\eta = 0.1$, we note that it can be shown (see Appendix A) that for $x = 0$, and for values $n\eta = 1/2$, except when $n = 1$, the strain becomes zero when $n$ is odd. This will occur at $\eta = (1/2/3 = 0.167)$, $(1/2/5 = 0.100)$, $(1/2/7 = 0.0714)$, and so on, and after the complete pulse is in the layer, the strain will be zero. The left side of Fig. 4 illustrates this by showing the displacements in the layer versus the dimensionless time $\tau = t \, \beta/2H$, for $n = 3$, 5, and 7. For these dimensionless
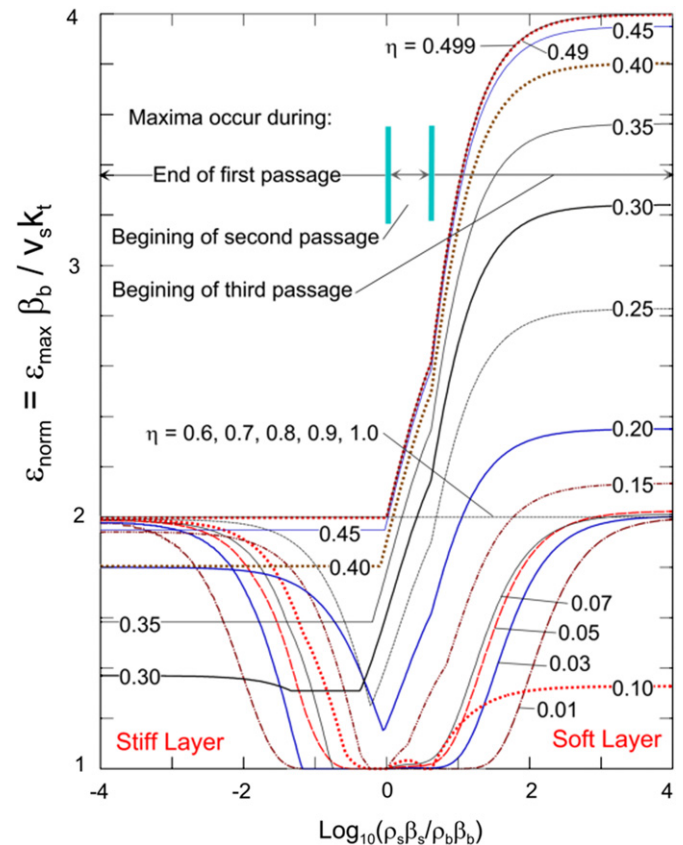


**Fig. 2.** Amplifications (1) at the end of the first passage $\overline{\varepsilon}_{1e}$, (2) at the beginning of the second passage $\overline{\varepsilon}_2$, and (3) at the beginning of the third passage $\overline{\varepsilon}_3$, plotted versus impedance ratio $r$.



**Fig. 3.** Normalized peak strain $\overline{\varepsilon}_{norm} = \varepsilon_{\max} \beta_b / v_s k_t$ versus impedance ratio $r = \rho_s \beta_s / \rho_b \beta_b$, for 19 example values of dimensionless frequencies $\eta$.
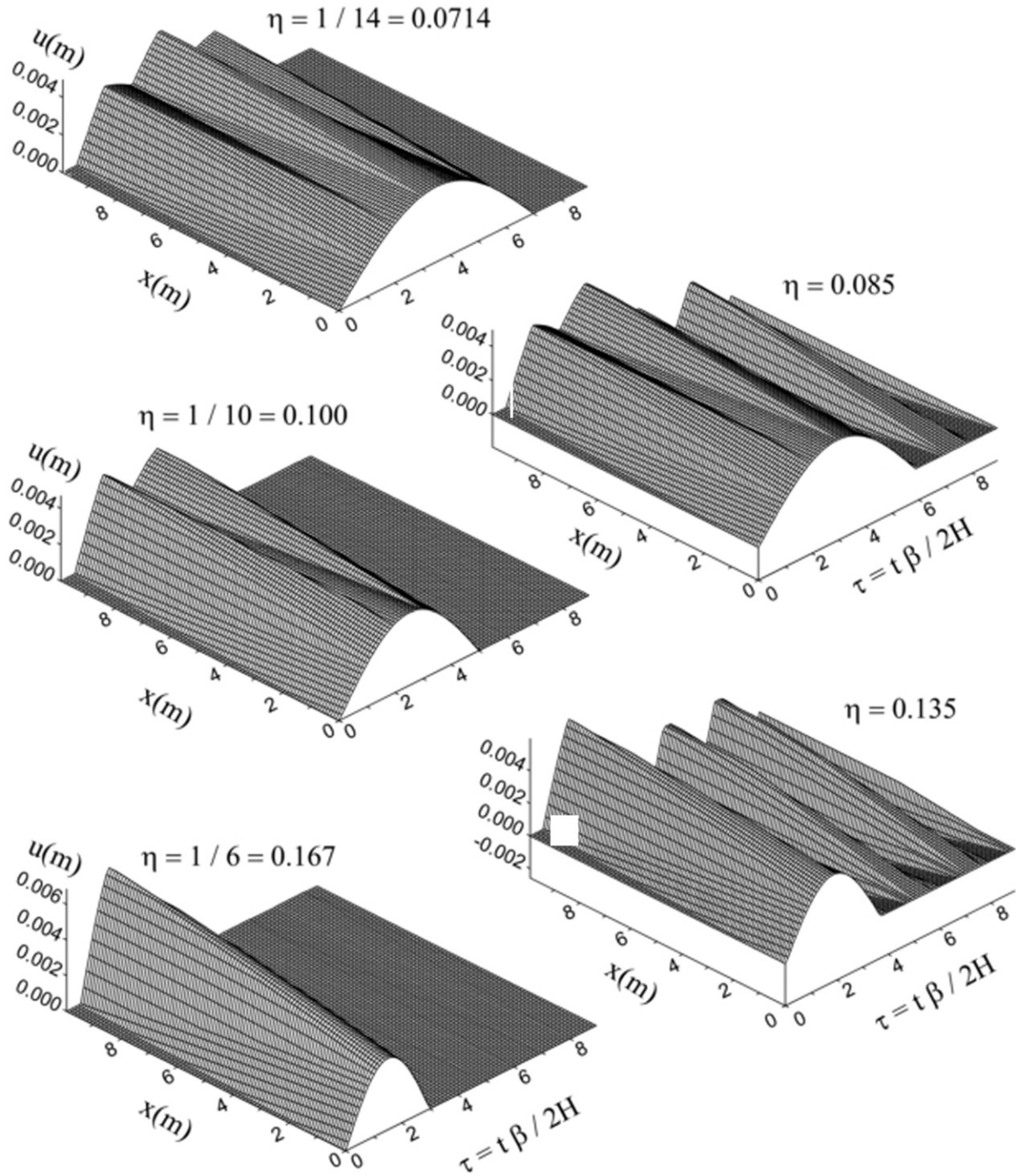
**Fig. 4.** Displacements along the thickness of the layer, $x$, versus normalized time $\tau = \beta_b t / 2H_b$, for nine passages ($\tau = 9$) bottom–top–bottom, and for five dimensionless frequencies $\eta = 0.0714$, 0.085, 0.100, 0135, and 0.167.

frequencies, the maximum amplification occurs before the pulse has completely entered the layer. Fig. 5 shows the normalized peak strains $\bar{\varepsilon}_{\max}$, the position where they occur $x(\bar{\varepsilon}_{\max})/H$, and the times when they occur $\beta_b\, t(\bar{\varepsilon}_{\max})/2H$, plotted versus $\eta = 1/2n$.

Next we examine the cases in which $r \to 0$, $k_r \to 1$ (left side of Fig. 3). We evaluate the amplification of the strain from Eq. (4) at $x = 0$, term by term, as

$$\bar{\varepsilon}(0,t) = -\cos\frac{\pi \cdot t}{t_d} + \cos\frac{\pi}{t_d}(t-t_1) - \cos\frac{\pi}{t_d}(t-t_1) + \cos\frac{\pi}{t_d}(t-2t_1)$$

$$-\cos\frac{\pi}{t_d}(t-2t_1) + \ldots + \cos\frac{\pi}{t_d}(t-n\cdot t_1). \tag{27}$$

All of the terms except the first and the last cancel out, and the amplification is

$$\bar{\varepsilon}(0,t) = \cos\frac{\pi \cdot t}{t_d}(t-n\cdot t_1) - \cos\frac{\pi \cdot t}{t_d} = -2\sin\frac{\pi}{2\cdot t_d}(2t-n\cdot t_1)\cdot\sin\frac{\pi}{2\cdot t_d}(-n\cdot t_1)$$

$$= 2\cdot\left(\sin\frac{\pi \cdot t}{t_d}\cdot\cos\frac{n\pi t_1}{2t_d} - \cos\frac{\pi \cdot t}{t_d}\cdot\sin\frac{n\pi t_1}{2t_d}\right)\cdot\sin\frac{n\pi\, t_1}{2t_d}. \tag{28}$$

Evaluating Eq. (28) at $t = t_d$, and remembering that $t_1/t_d = 2\eta$, we obtain

$$\bar{\varepsilon}(0,t) = 2\cdot\sin^2(n\pi\, t_1/2t_d) = 2\cdot\sin^2 n\eta\pi = 1-\cos 2n\eta\pi \tag{29}$$
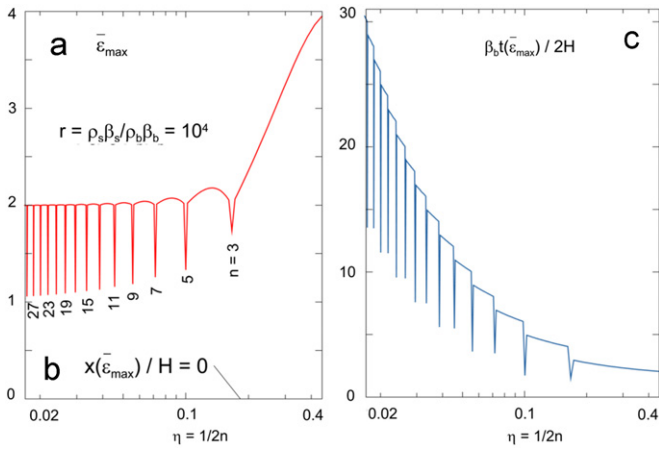
**Fig. 5.** (a) Amplification $\bar{\varepsilon}_{max}$, (b) at the base of the layer, and (c) the normalized time when it occurs, versus dimensionless frequency $\eta = 1/2n$, for impedance ratio $r = \rho_s \beta_s / \rho_b \beta_b = 10^4$.
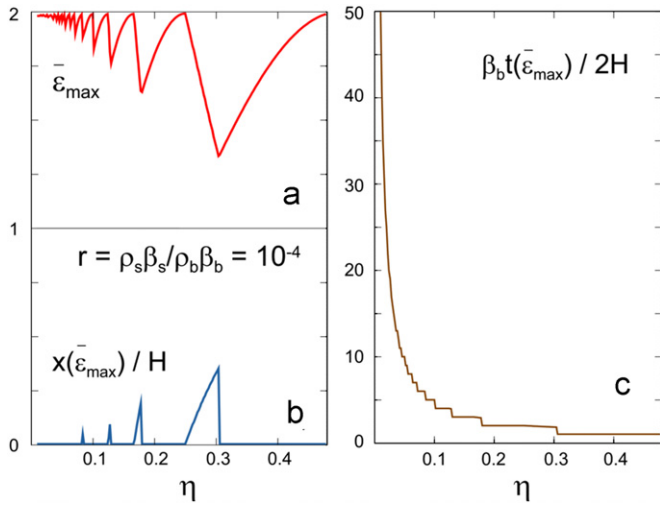


**Fig. 6.** (a) Amplification $\bar{\varepsilon}_{max}$, (b) normalized location where it occurs, and (c) the normalized time when it occurs, versus dimensionless frequency $\eta$, for impedance ratio $r = \rho_s \beta_s / \rho_b \beta_b = 10^{-4}$.

and

$$n = t_d/t_1 = (H/(\beta\eta))/(2H/\beta) = 1/(2\eta), \qquad (30)$$

which is the length of the pulse normalized by two heights of the layer, or the number of passages the pulse has traveled, until it is completely applied at $x=0$. Using Eq. (30) in Eq. (29), we obtain that the amplification of the strain as

$$\bar{\varepsilon}(0,t) = 2. \qquad (31)$$

This applies for long pulses ($\eta \to 0$, $\bar{\varepsilon}(0,t) \to 2$) and for pulses for which $n$ is an integer, so evaluating at time equal to the duration of the pulse, we evaluate strains at the point $x=0$. If the pulse is shorter and $n$ is not an integer, there is a departure from the amplification of 2. The maximum amplifications (the maximum normalized strains), their locations (normalized by the thickness of the layer), and their times (normalized by $t_1$) are shown in Fig. 6.

## 4. Discussion and conclusions

We described the amplification of half-sine shear-wave pulses propagating into a soil layer, with the objective of providing some understanding of the resulting response and how it depends upon the stiffness of the layer relative to the stiffness of the half space. We also defined the dimensionless limits for the wave amplitudes so that a linear strong-motion pulse in the half-space would remain linear as it continues to propagate into the layer, and until its energy is eventually dissipated through radiation back into the half space. We considered only linear, non-dissipating materials for both the layer and the half space.

For incident short pulses ($\eta > 0.5$), which lead to linear response of the layer, the amplification of the strain, with normalized pulse amplitude $\alpha(=A/(H_b \varepsilon_{yb}))$, which represents a normalized ratio of the average drift in the layer $A/H_b$ and of the yielding strain in the soil material $\varepsilon_{yb}$), is equal to 2. It results from interference of the strain of the up-propagating wave, with the strain from the wave reflected from the free layer surface and propagating downward. For long pulses ($\eta \leq 0.5$), the amplification of strains is more complicated and depends upon the impedance ratio between the half-space and the layer material. Depending upon the duration of the pulse, it can occur during first-, second-, or higher-order passes of the wave up and down the layer.

The principal contribution to the peak amplitudes of strong ground motion is associated with strong-motion peaks in arriving earthquake waves, which propagate coherently over large distances and dominate the peaks of the recorded ground acceleration, velocity, and displacement, the associated response spectra [20,21,23,34], and in the numerical simulations of strong motion accelerations [22,35]. For the development of design criteria of underground structures, it is also important to understand and describe how the peak strains in the soft surface deposits depend upon the local site characteristics and how their amplitudes are amplified by the local layer properties [11,30,12]. Observations of strong ground motion in the near field help in relating surface strain amplitudes to the observed impacts on man-made structures [31,32] and in the verification of the zoning and hazard maps that aim to predict the geographical distribution of the expected linear peak strains near the ground surface [19]. Characterization of the depths where the first peak strains occur also helps in understanding and interpreting the strong ground motion, which can lead to the soil liquefaction [24].

Mutatis mutandis, many results of this study can be applied to wide and not very tall buildings, which respond mainly in shear and which do not experience significant contributions to the response from the rocking component of soil-structure interaction. Because one of the principal design criteria is governed by the allowed maximum drift (average rotation of structural members between adjacent floors), and because the possible damage can be related directly to the exceeding of certain drift amplitudes [3,26,29] and to the wave motion in buildings in general [6], it is seen that the results we present in this paper for a layer of soil will apply also to the approximate, one-dimensional representation of the building response.

Starting with Eq. (16) and using Fig. 3 (which shows amplification of shear strain in the range 2–4, depending upon $\eta$), with the assumption that serious damage in a building will occur for drifts exceeding about 0.01 [3], if we neglect the effects of soil–structure interaction and assume that $k_t \sim 1$ (i.e., that $v_{lin} \sim v_{max}$, where $v_{max}$ is the peak ground velocity), we can compute an estimate of the peak ground velocity that will initiate damage from $v_{max} \sim 0.01\beta_b/\bar{\varepsilon}_{norm} = 0.01 \cdot 100(m/s) \cdot 100(cm/m)/(2 \text{ to } 4) = 25$ to $50 cm/s$. Here, we assumed that the velocity of shear waves in a building is about 100 m/s. Soil-structure interaction will act to diminish the free-fields peak ground velocity by scattering the incident waves from the foundation [25], but the transmission coefficient $k_t$, which will be greater than 1 (here we assumed $k_t \sim 1$), will amplify the incident-wave amplitude. In the above first-order approximation, we ignored both of these effects, yet in spite of these approximations it is seen why buildings get damaged in

the near field of strong earthquakes. The largest peak ground velocities recorded near moving faults so far are about 200 cm/s [26], or about one order of magnitude larger than the strong motions capable of damaging the structures.

## Appendix A

From Eq. (4), at arbitrary point A, and at time $t = t_d + \frac{x}{\beta} + \delta$ – that is, after the tail of the wave going upward has passed point A – in the first passage (the difference of the step functions for $j=1$ of the first term in Eq. (4) is 0), and remembering that $k_r \rightarrow -1$, we have

$$\varepsilon(x,t) = 0 + (-1)^0 \cos\frac{\pi}{t_d}\left(t-t_1+\frac{x}{\beta}\right) + (-1)^1\left[-\cos\frac{\pi}{t_d}\left(t-t_1-\frac{x}{\beta}\right)+\cos\frac{\pi}{t_d}\left(t-t_2+\frac{x}{\beta}\right)\right] + (-1)^2\left[-\cos\frac{\pi}{t_d}\left(t-t_2-\frac{x}{\beta}\right)+\cos\frac{\pi}{t_d}\left(t-t_3+\frac{x}{\beta}\right)\right]$$
$$+\ldots+(-1)^n\left[-\cos\frac{\pi}{t_d}\left(t-t_n-\frac{x}{\beta}\right)\right]$$

or

$$\varepsilon(x,t) = \cos\frac{\pi}{t_d}\left(t-t_1+\frac{x}{\beta}\right)+\cos\frac{\pi}{t_d}\left(t-t_1-\frac{x}{\beta}\right)-\cos\frac{\pi}{t_d}\left(t-t_2+\frac{x}{\beta}\right)-\cos\frac{\pi}{t_d}\left(t-t_2-\frac{x}{\beta}\right)+\cos\frac{\pi}{t_d}\left(t-t_3+\frac{x}{\beta}\right)+\cos\frac{\pi}{t_d}\left(t-t_3-\frac{x}{\beta}\right)$$
$$-\ldots+\cos\frac{\pi}{t_d}\left(t-t_n+\frac{x}{\beta}\right)-\cos\frac{\pi}{t_d}\left(t-t_n-\frac{x}{\beta}\right). \tag{A.1}$$

Using the trigonometric identity

$$\cos\alpha+\cos\theta = \cos(y+z)+\cos(y-z) = \cos y\cos z-\sin y\sin z+\cos y\cos z+\sin y\sin z = 2\cos y\cos z = 2\cos\frac{\alpha+\theta}{2}\cos\frac{\alpha-\theta}{2}, \text{ and taking}$$

$\alpha = \frac{\pi}{t_d}\left(t-t_i+\frac{x}{\beta}\right), \; \theta = \frac{\pi}{t_d}\left(t-t_i-\frac{x}{\beta}\right)$ and $t_k = k\cdot t_1$, we rewrite the Eq. as

$$\varepsilon(x,t) = 2\cos\frac{\pi(t-t_1)}{t_d}\cos\frac{\pi\cdot x}{\beta t_d}-2\cos\frac{\pi(t-t_2)}{t_d}\cos\frac{\pi\cdot x}{\beta t_d}+2\cos\frac{\pi(t-t_3)}{t_d}\cos\frac{\pi\cdot x}{\beta t_d}-\ldots+2\cos\frac{\pi(t-t_n)}{t_d}\cos\frac{\pi\cdot x}{\beta t_d}$$
$$= 2\cos\frac{\pi\cdot x}{\beta t_d}\left[\cos\frac{\pi(t-t_1)}{t_d}-\cos\frac{\pi(t-2t_1)}{t_d}+\cos\frac{\pi(t-3t_1)}{t_d}-\ldots+\cos\frac{\pi(t-3t_1)}{t_d}\right], \tag{A.2}$$

and using the identity $\cos(y-z)=\cos y\cos z+\sin y\sin z$ and regrouping cosine and sine terms, the last equation becomes

$$\varepsilon(x,t) = 2\cos\frac{\pi\cdot x}{\beta\cdot t_d}\left(\cos\frac{\pi\cdot t}{t_d}\cdot\cos\frac{\pi\cdot t_1}{t_d}-\cos\frac{\pi\cdot t}{t_d}\cdot\cos\frac{2\pi\cdot t_1}{t_d}+\cos\frac{\pi\cdot t}{t_d}\cdot\cos\frac{3\pi\cdot t_1}{t_d}-\ldots\ldots\right.$$
$$\left.+\sin\frac{\pi\cdot t}{t_d}\cdot\sin\frac{\pi\cdot t_1}{t_d}-\sin\frac{\pi\cdot t}{t_d}\cdot\sin\frac{2\pi\cdot t_1}{t_d}+\sin\frac{\pi\cdot t}{t_d}\cdot\sin\frac{3\pi\cdot t_1}{t_d}-\ldots\right)$$

$$\varepsilon(x,t) = 2\cos\frac{\pi\cdot x}{\beta\cdot t_d}\left(\cos\frac{\pi\cdot t}{t_d}(\cos\frac{\pi\cdot t_1}{t_d}-\cos\frac{2\pi\cdot t_1}{t_d}+\cos\frac{3\pi\cdot t_1}{t_d}-\ldots+\cos\frac{n\pi\cdot t_1}{t_d})\right.$$
$$\left.+\sin\frac{\pi\cdot t}{t_d}\left(\sin\frac{\pi\cdot t_1}{t_d}-\sin\frac{2\pi\cdot t_1}{t_d}+\sin\frac{3\pi\cdot t_1}{t_d}-\ldots+\sin\frac{n\pi\cdot t_1}{t_d}\right)\right). \tag{A.3}$$

We set

$$\pi t_1/t_d = (2\pi H/\beta)/(H/(\beta\eta)) = 2\pi\eta = \phi. \tag{A.4}$$

The first alternating sequence in Eq. (A.3) becomes

$$A_n = \cos\phi-\cos2\phi+\cos3\phi-\ldots+\cos n\phi, \tag{A.5a}$$

and the second becomes

$$B_n = \sin\phi-\sin2\phi+\sin3\phi-\ldots+\sin n\phi. \tag{A.5b}$$

Multiplying (A.5b) with $i = \sqrt{-1}$ and adding it to (A.5a), we obtain the complex sequence

$$A_n+iB_n = \cos\phi+i\sin\phi-(\cos2\phi+i\sin2\phi)+(\cos3\phi+i\sin3\phi)-\ldots+(\cos3\phi+i\sin3\phi). \tag{A.6}$$

Using the Moivre formula, $\cos k\phi+i\sin k\phi = e^{ik\phi} = (e^{i\phi})^k = (\cos\phi+i\sin\phi)^k$, and replacing $\cos\phi+i\sin\phi = z$, we find that (A.6) becomes

$$A_n+iB_n = z\cdot(1-z+z^2-\ldots+z^{n-1}). \tag{A.7}$$

For $n$ odd only

$$1+z^n = (1+z)(1-z+z^2-\ldots+z^{n-1}), \tag{A.8}$$

where the term in parenthesis in (A.7) is

$$1-z+z^2-\ldots+z^{n-1} = \frac{1+z^n}{1+z},$$

and, after replacing $z = \cos\phi + i\sin\phi$ and using the Moivre formula, (A.7) becomes

$$A_n + iB_n = (\cos\phi + i\sin\phi) \cdot \frac{1 + \cos n\phi + i\sin n\phi}{1 + \cos\phi + i\sin\phi}. \tag{A.9}$$

After using the identities

$$1 + \cos\phi = 2\cos^2\frac{\phi}{2} \quad \text{and} \quad \sin\phi = 2\sin\frac{\phi}{2}\cos\frac{\phi}{2} \tag{A.9}$$

becomes

$$A_n + iB_n = (\cos\phi + i\sin\phi) \cdot \frac{2\cos\frac{n\phi}{2}\left(\cos\frac{n\phi}{2} + i\sin\frac{n\phi}{2}\right)}{2\cos\frac{\phi}{2}\left(\cos\frac{\phi}{2} + i\sin\frac{\phi}{2}\right)} = \frac{\cos\frac{n\phi}{2}}{\cos\frac{\phi}{2}} \cdot \left[\cos\frac{(n+1)\phi}{2} + i\sin\frac{(n+1)\phi}{2}\right].$$

Finally, replacing $\phi = 2\pi\eta$ in the last expression, we get

$$A_n + iB_n = \frac{\cos n\eta\pi}{\cos\eta\pi} \cdot [\cos(n+1)\eta\pi + i\sin(n+1)\eta\pi],$$

so the sequences (A.5a) and (A.5b) are

$$A_n = \frac{\cos n\eta\pi}{\cos\eta\pi} \cdot \cos(n+1)\eta\pi \quad \text{and} \quad B_n = \frac{\cos n\eta\pi}{\cos\eta\pi} \cdot \sin(n+1)\eta\pi$$

With these values, the solution for the strain (Eq. A3) becomes

$$\varepsilon(x,t) = 2\cos\frac{\pi \cdot x}{\beta \cdot t_d}\left[\cos\frac{\pi \cdot t}{t_d} \cdot \frac{\cos n\eta\pi}{\cos\eta\pi} \cdot \cos(n+1)\eta\pi + \sin\frac{\pi \cdot t}{t_d} \cdot \frac{\cos n\eta\pi}{\cos\eta\pi} \cdot \sin(n+1)\eta\pi\right],$$

and, using the identity $\cos\alpha\cos\beta + \sin\alpha\sin\beta = \cos(\alpha - \beta)$,

$$\varepsilon(x,t) = 2\cos\frac{\pi \cdot x}{\beta \cdot t_d} \cdot \frac{\cos n\eta\pi}{\cos\eta\pi} \cdot \cos\left[\frac{\pi \cdot t}{t_d} - (n+1)\eta\pi\right], \tag{A.10}$$

where $n$ is the order number of a passage of the wave along the path bottom–top–bottom of the layer.

Evaluating Eq. only for odd $n$, we can see that for $n\eta = 1/2$, except when $n = 1$, the strain becomes zero after the complete pulse is in the layer (Fig. 4).

## References

[1] Aki K, Richards PG. Quantitative Seismology. San Francisco: W. H. Freeman and Co.; 1980.

[2] Ewing MW, Jardetsky WS, Press F. Elastic Waves in Layered Media. New York: McGraw-Hill Inc.; 1957.

[3] A., Ghobarah. On drift limits associated with different damage levels. In: Proceedings of the international workshop on performance-based seismic design, Bled, Slovenia, 2004. p. 321–332.

[4] Gičev V, Trifunac MD. Energy and power of nonlinear waves in a seven story reinforced concrete building. Indian Society of Earthquake Technology Journal 2007;44(1):305–23.

[5] Gičev V, Trifunac MD. Permanent deformations and strains in a shear building excited by a strong motion pulse. Soil Dynamics and Earthquake Engineering 2007;27(8):774–92.

[6] Gičev, V., and M.D. Trifunac. Rotations in a shear beam model of a seven-story building caused by nonlinear waves during earthquake excitation, Structural Control and Health Monitoring 2009;16:460–82.

[7] Gičev, V., and M.D. Trifunac. Transient and permanent rotations in a shear layer excited by strong earthquake pulses, Bulletin of the Seismological Society of America 2009;99(2B):1391–403.

[8] Kanai, K.. Some problems of seismic vibration of structures. In: Proceedings of the third world conference on earthquake engineering, New Zealand, Vol. II, 1965. p. 260–275.

[9] Kanai K. Engineering Seismology. Tokyo, Japan: Univ. of Tokyo Press; 1983.

[10] Kausel E, Manolis GD, editors. Wave Motion in Earthquake Engineering. WIT Press; 2000.

[11] Lee VW, Trifunac MD. Response of tunnels to indent SH-waves. Journal of Engineering Mechanics, ASCE 1979;105(4):643–59.

[12] Paolucci R, Smerzini C. Earthquake-induced transient ground strains from dense seismic networks. Earthquake Spectra 2008;24(2):453–70.

[13] Safak E. Discrete-time analysis of seismic site amplification. Journal of Engineering Mechanics, ASCE 1995;121(7):801–9.

[14] Safak E. Wave propagation formulation of seismic response of multi-story buildings. Journal of Structural Engineering, ASCE 1999;12(4):426–37.

[15] Safak E. Characterization of seismic hazards and structural response by energy flux. Soil Dynamics and Earthquake Engineering 2000;20(1-4):39–43.

[16] Sezawa K, Kanai K. Decay in the seismic vibration of a simple or tall structure by dissipation of their energy into the ground. Bulletin of Earth Research Institute 1935;XIII(Part 3):681–97.

[17] Sezawa K, Kanai K. Improved theory of energy dissipation in seismic vibrations on a structure. Bulletin of Earthquake Research Institute 1936;XIV(Part 2):164–8.

[18] Snieder R, Safak E. Extracting the building response using interferometric imaging: theory and application to Millikan Library in Pasadena California. Bulletin of Seismological Society of America 2006;96(2):586–98.

[19] Todorovska MI, Trifunac MD. Hazard mapping of normalized peak strain in soil during earthquakes—microzonation of a metropolitan area. Soil Dynamics and Earthquake Engineering 1996;15(5):321–9.

[20] Todorovska MI, Trifunac MD. Distribution of pseudo spectral velocity during Northridge, California earthquake of 17 January, 1994. Soil Dynamics and Earthquake Engineering 1997;16(3):173–92.

[21] Todorovska MI, Trifunac MD. Amplitudes, polarity and time of peaks of strong ground motion during the 1994 Northridge, California earthquake. Soil Dynamics and Earthquake Engineering 1997;16(4):235–58.

[22] Trifunac MD. Method for synthesizing realistic strong ground motion. Bulletin of Seismological Society of America 1971;61(6):1739–53.

[23] Trifunac MD. Dependence of Fourier spectrum amplitudes of recorded earthquake accelerations on magnitude, local soil conditions and depth of sediments. Earthquake Engineering and Structural Dynamics 1989;18(7):999–1016.

[24] Trifunac MD. Empirical criteria for liquefaction in sands via standard penetration tests and seismic wave energy. Soil Dynamics and Earthquake Engineering 1995;14(6):419–26.

[25] Trifunac, M.D. (2005). Power design method. In: Proceedings of earthquake engineering in the 21st century to mark 40th anniversary of IZIIS—Skopje, Keynote lecture, August 28–September 1, 2005, Skopje and Ohrid, Macedonia.

[26] Trifunac MD. The role of strong motion rotations in the response of structures near earthquake faults. Soil Dynamics and Earthquake Engineering 2008;29(2):382–93.

[27] Trifunac MD, Ivanović SS. Recurrence of site-specific response in former Yugoslavia – Part I: Montenegro. Soil Dynamics and Earthquake Engineering 2003;23(8):637–61.

[28] Trifunac MD, Ivanović SS. Reoccurrence of site-specific response in former Yugoslavia – Part II: Friuli, Banja Luka, and Kopaonik. Soil Dynamics and Earthquake Engineering 2003;23(8):663–81.

[29] Trifunac, M.D., and S.S. Ivanović (2003c). Analysis of drifts in a seven-story reinforced concrete structure, Dept. of Civil Eng. Report No. *CE 03-01,* Univ. of Southern California, Los Angeles, California.

[30] Trifunac MD, Lee VW. Peak surface strains during strong earthquake motions. Soil Dynamics and Earthquake Engineering 1996;15(5):311–9.

[31] Trifunac MD, Todorvska MI. Northridge, California, earthquake of 17 January 1994: density of pipe breaks and surface strains. Soil Dynamics and Earthquake Engineering 1997;16(3):193–207.

[32] Trifunac MD, Todorovska MI, Ivanović SS. Peak velocities, and peak surface strains during Northridge, California, earthquake of 17 January 1994. Soil Dynamics and Earthquake Engineering 1996;15(5):301–10.

[33] Trifunac MD, Hao TY, Todorovska MI. On reoccurrence of site-specific response. Soil Dynamics & Earthquake Engineering 1999;18(8):569–92.

[34] Udwadia FE, Trifunac MD. Characterization of response spectra through statistics of oscillator response. Bulletin of Seismological Society of America 1974;64(1):205–19.

[35] Wong HL, Trifunac MD. Generation of artificial strong motion accelerograms. Earthquake Engineering and Structural Dynamics 1979;7(6):509–27.